Effects of the water level on the flow topology over the Bolund island

A Cuerva-Tejero[1], T S Yeow[1], C Gallego-Castillo[2], O Lopez-Garcia[1]

[1] Instituto Universitario de Microgravedad Ignacio Da Riva, E.T.S.I. Aeronáuticos, Universidad Politécnica de Madrid, E-28040 Madrid, Spain
[2] Departamento de Vehículos Aeroespaciales, E.T.S.I. Aeronáuticos, Universidad Politécnica de Madrid, E-28040 Madrid, Spain

E-mail: `alvaro.cuerva@upm.es`

Abstract.
We have analyzed the influence of the actual height of Bolund island above water level on different full-scale statistics of the velocity field over the peninsula. Our analysis is focused on the database of 10-minute statistics provided by Risø-DTU for the Bolund Blind Experiment. We have considered 10-minute periods with near-neutral atmospheric conditions, mean wind speed values in the interval [5,20] m/s, and westerly wind directions. As expected, statistics such as speed-up, normalized increase of turbulent kinetic energy and probability of recirculating flow show a large dependence on the emerged height of the island for the locations close to the escarpment. For the published ensemble mean values of speed-up and normalized increase of turbulent kinetic energy in these locations, we propose that some ammount of uncertainty could be explained as a deterministic dependence of the flow field statistics upon the actual height of the Bolund island above the sea level.

1. Introduction

The Bolund Experiment, conducted by Risø-DTU on the Bolund peninsula in Denmark during a 3-month period in the winter of 2007-2008 ([1], [2]), is a well-known reference case for benchmarking numerical and physical modelling of flows over complex terrain in neutral conditions without Coriolis effects. From an experimental point of view, the Bolund experiment is a field campaign that provides a unique dataset that includes cup and ultrasonic anemometer measurements (at different masts and at different heights), lidar scans, stability measurements and water level measurements. The experiment was designed as a blind comparison of different numerical flow models (including linear, RANS and LES) and also physical models (wind tunnel and water channel models) [3]. The main conclusions from the initial analysis of the experiment were: a) a great deal of scatter exists among the different numerical models (mainly in the vicinity of the island escarpment); b) the mean speed, S, is better predicted than turbulent kinetic energy, k; and c) the best models predicting both mean wind speed and turbulent kinetic energy (hereafter denoted TKE) are the RANS models with two closure equations [3].

One of the main geometric characteristics of Bolund is the escarpment facing approximately wind directions 200° to 295°(see figure 1, where northerly winds correspond to 0° and easterly winds correspond to 90°). It can be idealized as a combination of a 50° slope ramp extending from the sea bed up to $0.5H$, plus an almost vertical step from $0.5H$ up to H, where H is the
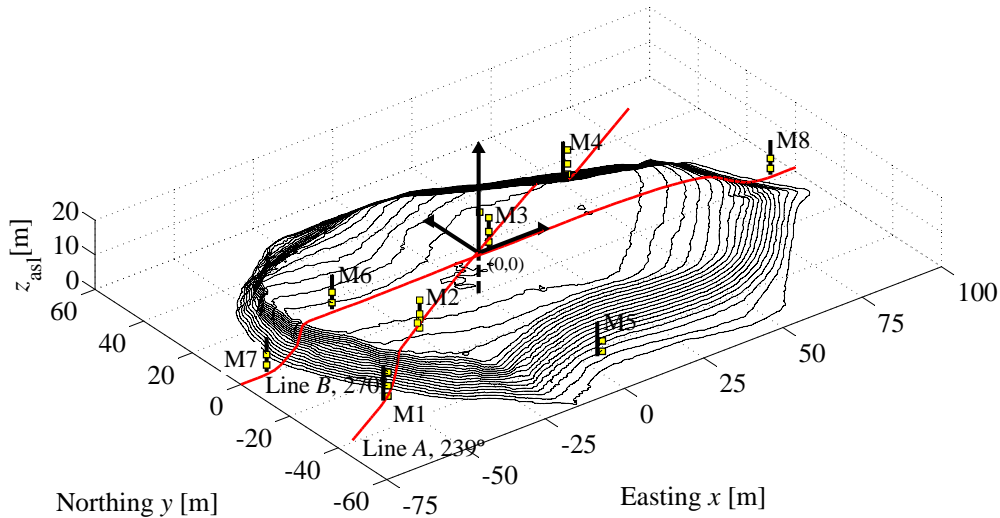
**Figure 1.** Masts locations in the Bolund experiment. The reference mast M0 is located in coordinates $[-181.1\,\mathrm{m}, -101.7\,\mathrm{m}]$ not shown in the figure. Ultrasonic anemometers: yellow squares. The Bolund reference system is indicated in the figure.

maximum height of the island above the sea bed. The escarpment height varies slightly in the interval 200°-295°, this being roughly equal to the maximum height of the island ($H = 11.79\,\mathrm{m}$ above the sea bed, see figure 2). This geometry guarantees that flow detaches at the edge (with a sufficiently large Reynolds number) while the flat top ensures reattachment of the flow on the island [4]. For westerly winds (Line B in the Bolund experiment jargon, see figure 1), both full-scale and wind tunnel analyse have shown that instantaneous detatchment-recirculation patterns take place intermittently at the edge of the escarpment but not often enough to significantly affect the mean velocity field. The flat top of the island extends downstream about 10 times the height of the island, ending with a slope down ramp of about $-40°$, where intermittent detatchment again takes place [4].

Another particular aspect of this test case is that the water height above the sea bed, h_S, changes with time. The variation is roughly on the order of $0.1H$, leading to a time variation of the emerged height of the island, which is likely to influence the flow topology over Bolund. In the blind experiment, Risø-DTU proposed to analyze the case corresponding to the day when the topography of the island was scanned by an airborne laser device (actually, the topography was scanned on two different days), resulting in a water level above the sea bed $h_S \simeq 0.75\,\mathrm{m}$ and a maximum height of the island above the sea level $h \simeq 11.04\,\mathrm{m}$. Obviously, it holds that $h = H - h_S$, as schematized in figure 2. To the authors' knowledge, the published results (both from numerical and physical models, authors' included) correspond to this situation, and the published full-scale results [2] which are the ones proposed by Risø-DTU for comparison purposes, correspond to $h = 11.04 \pm 0.4\,\mathrm{m}$.

2. Approach

We have re-analyzed the Bolund 10-minute database and performed a parametric analysis of the statistics of the velocity field versus the actual maximum height h of the island above the sea level, in order to determine the influence of such a height into the flow field statistics. We have considered 10-minute periods corresponding to the 270° wind direction (10-minute mean wind direction values in the interval [260°,280°], slightly wider than the interval [262°,278°] analyzed
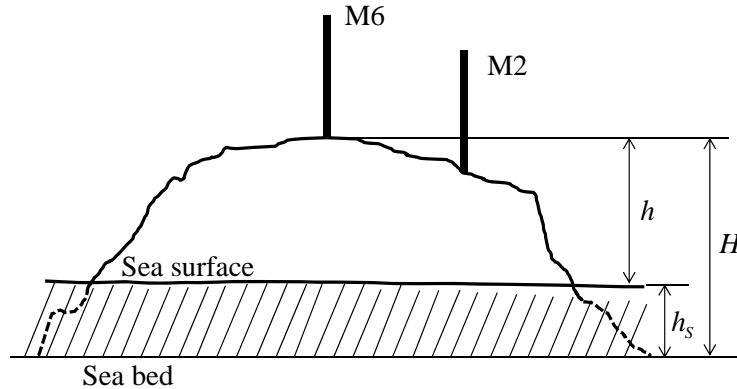
Figure 2. Definition maximum height of the island above the sea bed, H, maximum height of the island above the sea level, h, and water level above the sea bed, h_S. Schematic view from West.

Mast	x [m]	y [m]	Ground level [m]
M0	-181.7	-101.7	0.8
M7	-66.9	1.8	0.8
M3	3.2	1.8	11.7
M6	-46.1	2	11.4
M8	92.0	1.7	2.0

Table 1. Mast coordinates. x and y coordinates are expressed in the reference system of figure 1. Ground level means height of the mast base above sea bed. From [5].

in case 1 from [3]), with mean speed values in the interval [5,20] m/s and absolute values of the Obukhov length $|L| > 250$ m. We have classified the 10-minute periods in terms of the corresponding height above the sea level h, using 50% overlapping bins for the h values with a width $\Delta h = 0.3$ m and the bin-average of all the values within each bin has been performed. We have used overlapping bins to increase the number of bin-averaged values. Eight bins were obtained, with bin-averaged values of h ranging from 10.92 m to 11.89 m, using a N_{min} of three 10-minute periods per bin and typically a number of 10-minute periods per bin $N > 50$. The number of 10-minute periods per bin is shown in figure 3. It should be noted that the number of recorded 10-minute periods for the sensor at 2 m at M6 was smaller in the original data base. The same filtering criteria have been applied to all sensors.

Wind velocity measurements from ultrasonic anemometers at mast M7 at the foot of the escarpment, mast M6 just about $1H$ downstream of the escarpment, mast M3 about $5H$ downstream of the escarpment and at the mast M8 on the lee side of the island (fully immersed in the wake) have been analyzed (see figure 1 and table 1 to identify the mast locations). The calculated bin-averaged statistics are: a) the speed-up S/S_0, b) the normalized increase of TKE Δk, as defined in [3], c) the normalized variance of the longitudinal component of the wind velocity $\overline{u^2}/u_0^2$, d) the normalized turbulent shear stress $\overline{uw}/u_*^2$, (u_* being the friction velocity calculated as $u_* = |\overline{uw}_0|^{0.5}$ with $\overline{uw}_0$ the upwind turbulent shear stress from reference mast M0 at $z = 5$ m), and e) the probability $P(U_{10} + u_{10} < 0)$ of occurrence of instantaneous negative values of the longitudinal component $U_{10} + u_{10}$ (here we use U_{10} to refer to the 10-minute average and u_{10} to the corresponding instantaneous fluctuation) of the wind velocity. To obtain this probability we have assumed that the instantaneous values of such a velocity component
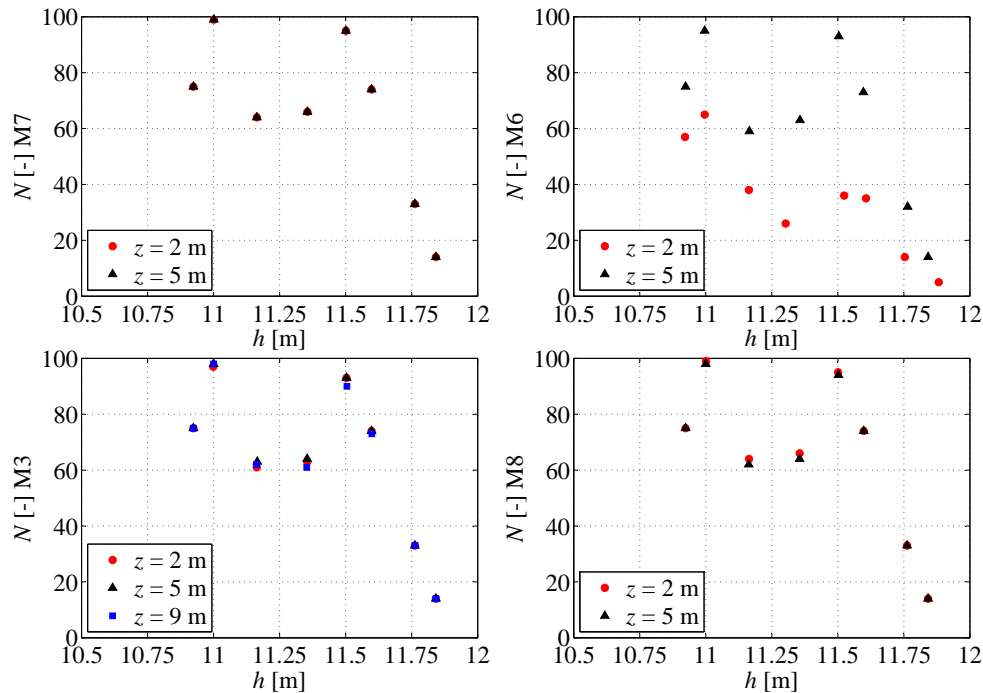
Figure 3. Number of 10-minute periods within each bin h, N, at M7, M6, M3 and M8. See figure 1 to identify mast locations. z: height above ground level of the sensor. Results for $270°$ wind direction (line B).

are normally distributed around the 10-minute mean (as suggested in [2]), so the mentioned probability is easily obtained from the 10-minute sample mean and variance. In all cases we have used a wind horizontal reference system (denoted "windvec2d" in [5]) which is a right-handed coordinate system, with the x axis aligned with the 10-minute horizontal mean velocity and the z axis is the upward vertical. In the case of the speed-up, the reference value, S_0, is estimated at the same height above ground level as the corresponding measurement over the island, S, by using a logarithmic law of the wall as proposed in [3]. For all other quantities the "0" subscript refers to measurements at $z = 5\,\mathrm{m}$ from the westerly upwind reference mast M0.

3. Analysis
As expected, the wind velocity measurements at lower heights at the mast M6 close to the escarpment show a great dependence on the actual height of the island above the sea level. This is evident in figure 4 where the bin-averaged values of the speed-up, S/S_0, are shown.

For instance, at $z = 2\,\mathrm{m}$ above ground level in M6, for the mentioned $270°$ wind direction case, the speed-up ranges linearly from $S/S_0 = 0.98$ for $h = 10.92\,\mathrm{m}$ down to $S/S_0 = 0.49$ for $h = 11.89\,\mathrm{m}$. The presented result is coherent, since a larger value of the actual height of the island above the sea level means a lower value of the actual ratio z/h of the measurement point, so the ultrasonic anemometer is closer to the ground in island height units, so the point is deeper immersed in the intermittent recirculation region generated at the escarpment edge. The sensor gets in and leaves the shear layer generated at the escarpment as h changes. Considering this argument, an augmentation of the normalized TKE (Δk) is expected as h increases; this is found in figure 5. For the location closest to the escarpment (M6, $z = 2\,\mathrm{m}$) the normalized increase of TKE ranges from $\Delta k = 0.1$ for $h = 10.92\,\mathrm{m}$ up to $\Delta k = 0.13$ for $h = 11.75\,\mathrm{m}$. In [6] it is
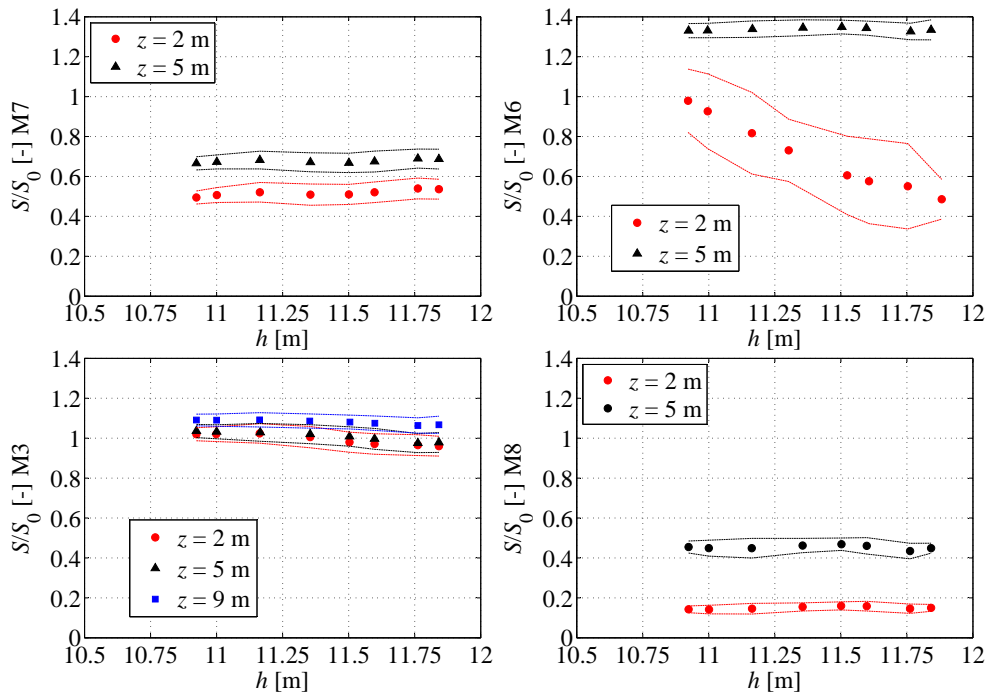
Figure 4. Speed-up, S/S_0, versus the maximum height of the island above sea level, h, at different heights at M7, M6, M3 and M8. Lines represent $\pm$rms intervals. Coding as in figure 3.
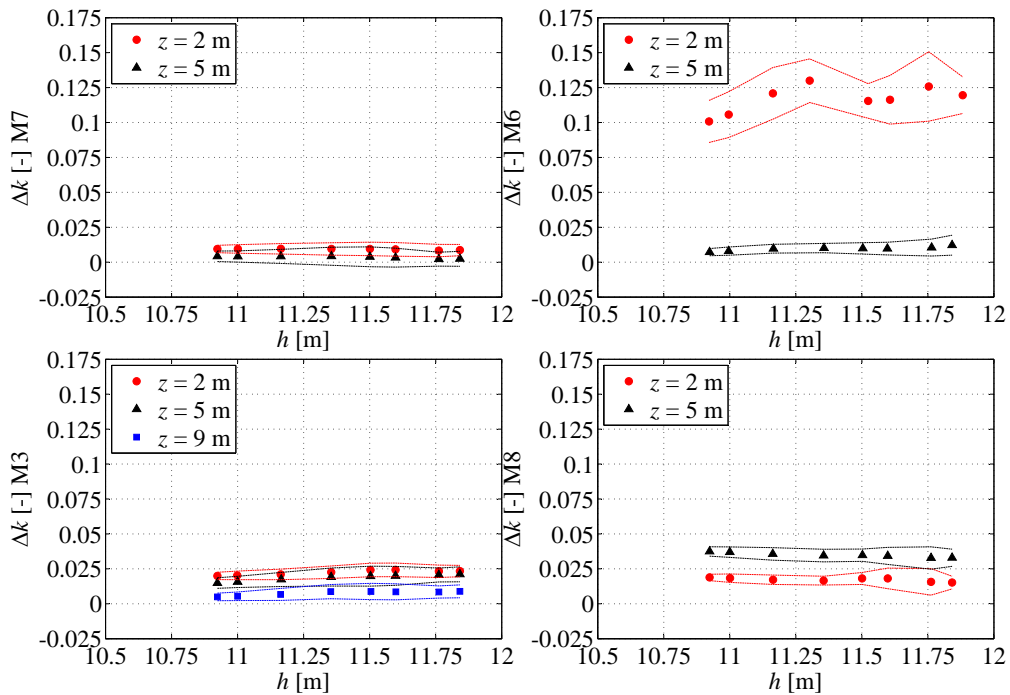
Figure 5. Normalized increase of TKE, Δk versus height of the island above sea level h at different heights at M7, M6, M3 and M8. Lines represent $\pm$rms intervals. Coding as in figure 3.
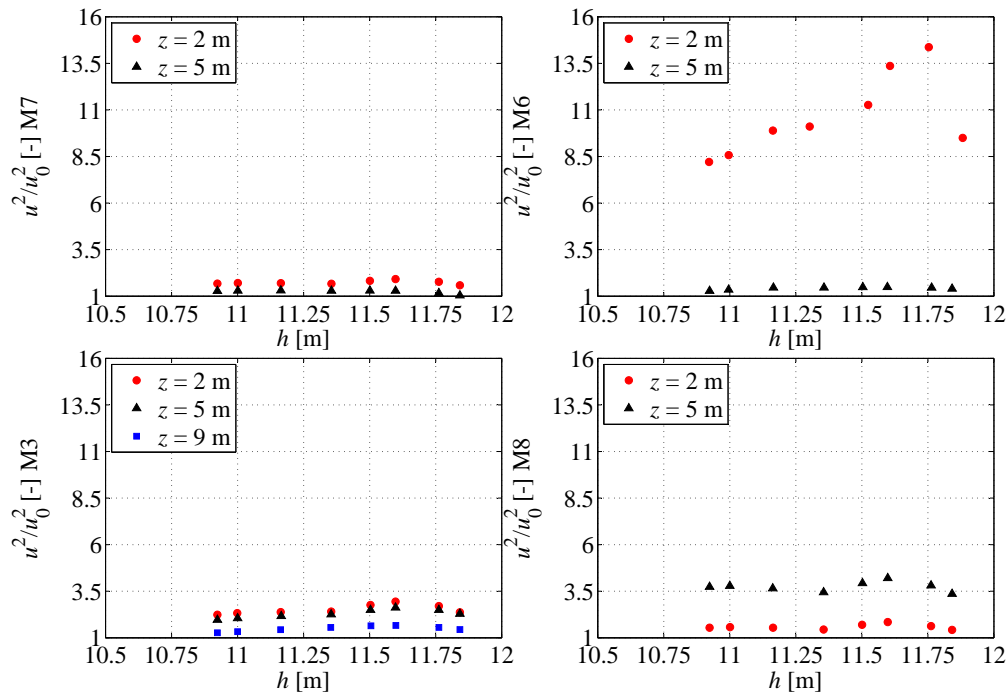
Figure 6. Variance of the longitudinal velocity component, $\overline{u^2}$, normalized with the corresponding value in the upstream undisturbed reference position M0, $\overline{u_0^2}$, versus the height of the island above sea level h, at different heights at M7, M6, M3 and M8. Coding as in figure 3.

shown that at this location a very large scatter of the 10-minute means for S/S_0 and Δk exists. Here, we propose that a part of this scatter can be explained as a deterministic dependence of the referred flow field statistics on the actual height of the Bolund island above the sea level, as shown in figures 4 and 5.

The variance of the longitudinal velocity component normalized with the corresponding value in the upstream undisturbed reference position (M0) ranges from $\overline{u^2}/\overline{u_0^2} = 8.23$ for $h = 10.92\,\mathrm{m}$ up to $\overline{u^2}/\overline{u_0^2} = 14.44$ for $h = 11.75\,\mathrm{m}$, as is shown in figure 6.

We also quantified the expected influence of the actual height of the island above the sea level, h, on the probability of recirculation; that is, the probability of having negative instantaneous values of the longitudinal component of the velocity, $P(U_{10} + u_{10} < 0)$. The probability of recirculation versus h is shown in figure 7. This probability ranges linearly from 1.5% for $h = 10.92\,\mathrm{m}$ up to 12% for $h = 11.75\,\mathrm{m}$ at $z = 2\,\mathrm{m}$ position in M6. This strong dependence is not found in the velocity measurements of the ultrasonic anemometer located at $z = 5\,\mathrm{m}$ at the referred mast M6, indicating that the point $z = 5\,\mathrm{m}$ is far enough from the intermittent recirculation region and the shear layer evolving above it, regardless of the water level variations. Therefore at this point, the speed-up, the normalized increase of TKE, and the non-dimensional variance of the longitudinal component of the wind velocity show little variation, and the probability of instantaneous recirculation is zero for all values of h. We have also quantified a variation of the normalized turbulent shear stress from -10 down to -28 at the mast M6 at $z = 2\,\mathrm{m}$.

In the case of the mast in the middle of the plateau, M3, the influence of h is weaker at $z = 2\,\mathrm{m}$ and $z = 5\,\mathrm{m}$, both in the speed-up and the normalized variance of the longitudinal component. For instance at $z = 2\,\mathrm{m}$ the speed-up decreases from $S/S_0 = 1.02$ for $h = 10.92\,\mathrm{m}$
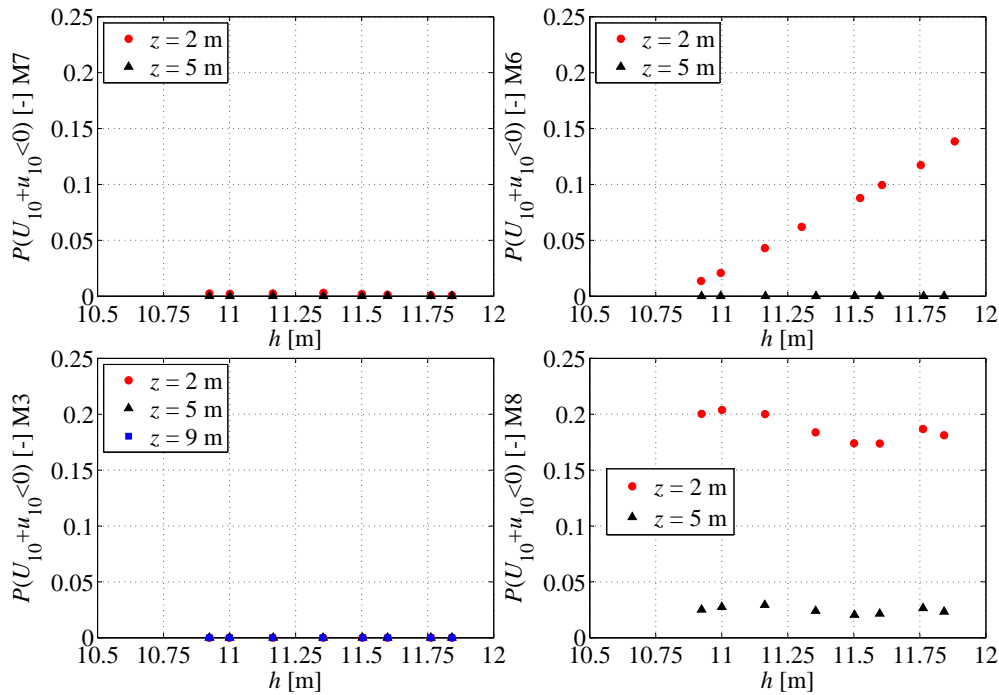
Figure 7. Probability of having negative instantaneous values of the longitudinal component of the velocity, $P(U_{10} + u_{10} < 0)$, versus height of the island above sea level h at different heights at M7, M6, M3 and M8. Coding as in figure 3.

down to $S/S_0 = 0.96$ for $h = 11.84\,\mathrm{m}$ and the normalized increase of TKE varies from 0.02 up to 0.023 for the same variation of the actual maximum height of the island above the sea level. This indicates that the higher deceleration and TKE increase originated at low heights at the escarpment when h is large, is still detected downstream on the plateau although highly mitigated.

The results for M8 located on the lee side wake of the island show a small increase in the speed-up (in the interval [0.14,0.16] and [0.43,0.47] for $z = 2\,\mathrm{m}$ and $z = 5\,\mathrm{m}$ respectively) and in the normalized variance of the longitudinal component of the wind speed at both heights. In the case of the probability of recirculation, a slight decrement of $P(U_{10} + u_{10} < 0)$ versus h is observed for $z = 2\,\mathrm{m}$ (from 20.38% down to 17.4%). Similarly in figure 8, more and more negative values of the turbulent shear stress are observed at the mentioned position as h increases. This situation is interpreted as follows: higher values of h at the escarpment produce stronger disturbance in the flow, therefore, as h increases larger levels of TKE and more negative values of $\overline{uw}$ are generated in the boundary layer closer to the ground ($z = 2\,\mathrm{m}$). Stronger turbulent shear stress at M8 is associated with higher entrainment of faster flow from above which leads to slightly lower values of probability of recirculation and slightly higher values of speed-up on the lee side.
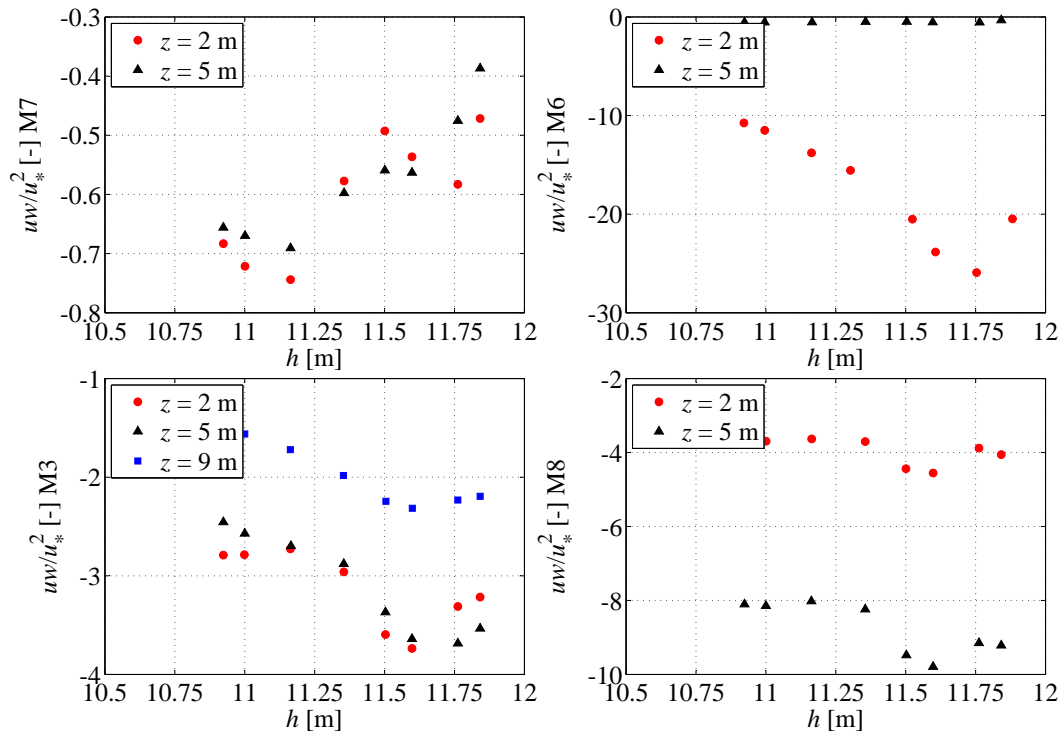
Figure 8. Turbulent shear stress, $\overline{uw}$, normalized with the friction velocity squared at the reference position M0, $u_* = |\overline{uw}_0|^{0.5}$ at $z = 5\,\text{m}$, versus height of the island above sea level h at different heights at M7, M6, M3 and M8. Coding as in figure 3.

4. Conclusions

Broadly speaking, the influence of the actual sea level is more noticeable close to the escarpment. This effect leads, at those locations, to a large dependence of the bin-averaged statistics of wind velocity on the actual maximum height of the island above the sea level. The larger the value of the mentioned maximum height, the larger the effect of recirculation and generation of TKE at low heights close to the escarpment. These effects are also detected in the middle of the plateau. However, larger values of the emerged height of the island also leads to larger magnitudes of the turbulent shear stress, which likely produces a more intense entrainment of higher speed flow from upper regions, producing less intense deceleration and lower probability of recirculation on the lee side. We have proposed that part of the scatter associated with the statistics of available full-scale measurements at low height close to the Bolund escarpment, can be explained as a deterministic dependence of these statistics on the emerged height of the island.

5. Acknowledgements

References

[1] Bechmann A, Johansen J and Sørensen N N 2007 The Bolund Experiment - Design of Measurement Campaign using CFD Tech. Rep. Risø-R-1623(EN) Risø

[2] Berg J, Mann J, Bechmann A, Courtney M S and Jørgensen H E 2011 *Boundary-Layer Meteorology* **141** 219–243. DOI: 10.1007/s10546–011–9636–y

[3] Bechmann A, Sørensen N N, Berg J, Mann J and Rethore P E 2011 *Boundary-Layer Meteorology* **141** 219–243. DOI: 10.1007/s10546–011–9637–x

[4] Yeow T S, Cuerva A and Pérez J 2013 *Wind Energy* DOI: 10.1002/we.1688

[5] Bechmann A, Berg J, Courtney M S, Jørgensen H E, Mann J and ørensen N N 2009 The Bolund Experiment: Overview and Background Tech. Rep. Risø-R-1658(EN) Risø

[6] Bechmann A 2010 Presentations from "The Bolund Experiment: Workshop" 3-4th December 2009 Tech. Rep. Risø-R-1745(EN) Risø